

DEVELOPMENTAL BIOLOGY

Fructose-1,6-bisphosphate prevents pregnancy loss by inducing decidual COX-2⁺ macrophage differentiation

Wen-Jie Zhou^{1,2,3,†}, Hui-Li Yang^{1,†}, Jie Mei⁴, Kai-Kai Chang¹, Han Lu^{1,3}, Zhen-Zhen Lai¹, Jia-Wei Shi¹, Xiao-Hui Wang³, Ke Wu¹, Tao Zhang⁵, Jian Wang¹, Jian-Song Sun⁶, Jiang-Feng Ye⁷, Da-Jin Li¹, Jian-Yuan Zhao^{8*}, Li-Ping Jin^{3*}, Ming-Qing Li^{1,9*}

Decidualization is an intricate biological process in which extensive remodeling of the endometrium occurs to support the development of an implanting blastocyst. However, the immunometabolic mechanisms underlying this process are still largely unknown. We found that the decidualization process is accompanied by the accumulation of fructose-1,6-bisphosphate (FBP). The combination of FBP with pyruvate kinase M stimulated IL-27 secretion by endometrial stromal cells in an ERK/c-FOS-dependent manner. IL-27 induced decidual COX-2⁺ M2-like macrophage differentiation, which promotes decidualization, trophoblast invasion, and maternal-fetal tolerance. Transfer of *Ptgs2*⁺/COX-2⁺ macrophages prevented fetal loss in *Il27ra*-deleted pregnant mice. FBP levels were low in plasma and decidual tissues of patients with unexplained recurrent spontaneous abortion. In therapeutic studies, FBP supplementation significantly improved embryo loss by up-regulation of IL-27-induced COX-2⁺ macrophage differentiation in a mouse model of spontaneous abortion. These findings collectively provide a scientific basis for a potential therapeutic strategy to prevent pregnancy loss.

INTRODUCTION

Decidualization refers to the transformation that the stromal compartment of the endometrium must undergo a series of adaptations to accommodate a successful pregnancy (1). Deficiencies in decidualization are associated with pregnancy complications and reproductive diseases, including female infertility, spontaneous abortion, intra-uterine growth restriction (IUGR), and preeclampsia (1–3). Decidualization occurs, both in vitro and in vivo, in response to ovarian steroid hormones (estradiol and progesterone) and embryo implantation, which is characterized by the transformation of endometrial stromal cells (ESCs) from fibroblast-like cells into large polygonal decidual stromal cells (DSCs) that are rich in cytoplasmic glycogen and lipid droplets (1, 4). Unfortunately, the regulatory and functional mechanisms of decidualization still remain largely unknown. Reproductive failure, especially when recurrent, is a frustrating and

challenging area for health care providers because of limited evidence-based treatments. Despite significant advances in preimplantation genetic tests, implantation failure and miscarriage cannot be effectively prevented. The in-depth understanding of decidualization provides an opportunity to open an avenue for the development of therapeutic targets and strategies.

Generalized decidualization also includes secretion from the endometrial glandular epithelium, remodeling of the uterine spiral artery, enrichment and redistribution of immune cells, and change of extracellular matrix components (5, 6). Decidual macrophages (dMφs), the second largest leukocyte population (approximately 20%) found in uterine mucosa (decidua) during pregnancy, are involved in multiple processes required for a successful pregnancy, including fetal-maternal tolerance, trophoblast invasion, as well as tissue and vascular remodeling (7). Specific depletion of macrophages results in implantation failure and increased rates of fetal loss in mice (8, 9). Macrophages are highly plastic and heterogeneous cells (10). During the different phases of gestation, macrophages undergo dynamic changes on the basis of environmental stimuli and mediators, differentiating to neither the classic M1 nor M2 subset (11, 12). Accumulating evidence has indicated that M2 macrophages are the predominant phenotype in the decidua of early pregnancy (9, 13). However, the molecular mechanisms underlying the activation and functions of dMφs are still largely unknown.

Recently, metabolic reprogramming has been reported to be directly involved in the differentiation and functional regulation of macrophages (14–16). Therefore, this study aimed to investigate the characteristics and regulatory mechanisms of hormone-metabolism-macrophage differentiation in decidualization, its pathogenic role in pregnancy loss, and potential intervention strategies both in vitro and in vivo.

RESULTS

Fructose-1,6-bisphosphate accumulation during decidualization

To observe the metabolite profiles of decidualization in Chinese individuals, 12 healthy control endometrium from the secretory

¹Laboratory for Reproductive Immunology, NHC Key Lab of Reproduction Regulation (Shanghai Institute of Planned Parenthood Research), Hospital of Obstetrics and Gynecology, Shanghai Medical School, Fudan University, Shanghai 200080, People's Republic of China. ²Reproductive Medical Center, Department of Obstetrics and Gynecology, Ruijin Hospital, Shanghai Jiao Tong University School of Medicine, Shanghai 200025, People's Republic of China. ³Clinical and Translational Research Center, Shanghai First Maternity and Infant Hospital, Tongji University School of Medicine, Shanghai 200040, People's Republic of China. ⁴Reproductive Medicine Center, Department of Obstetrics and Gynecology, Nanjing Drum Tower Hospital, The Affiliated Hospital of Nanjing University Medicine School, Nanjing 210000, People's Republic of China. ⁵Assisted Reproductive Technology Unit, Department of Obstetrics and Gynecology, Faculty of Medicine, Chinese University of Hong Kong, Hong Kong, People's Republic of China. ⁶National Research Centre for Carbohydrate Synthesis, Jiangxi Normal University, Nanchang, Jiangxi Province 330022, People's Republic of China. ⁷Division of Obstetrics and Gynecology, KK Women's and Children's Hospital, Singapore 229899, Singapore. ⁸State Key Laboratory of Genetic Engineering, Collaborative Innovation Center for Genetics and Development, School of Life Sciences, Fudan University, Shanghai 200433, People's Republic of China. ⁹Shanghai Key Laboratory of Female Reproductive Endocrine Related Diseases, Hospital of Obstetrics and Gynecology, Shanghai Medical School, Fudan University, Shanghai 200080, People's Republic of China.

*Corresponding author. Email: mqli@fudan.edu.cn (M.-Q.L.); jinlp01@163.com (L.-P.J.); zhaojy@fudan.edu.cn (J.-Y.Z.)

†These authors contributed equally to this work.

phase and 12 decidua tissues from normal pregnancy were recruited. Metabolomics results revealed 63 differential metabolites between primary cultured ESCs and DSCs, especially the metabolites of glycometabolism [i.e., the accumulation of fructose-1,6-bisphosphate (FBP)] (Fig. 1A). Expression of various enzymes involved in glycometabolism in the DSC group changed relative to that in the secretary ESCs (Fig. 1, B and C). In particular, increased levels of hexokinase 1 (HK1) and phosphofructokinase 1 (PFK1) and decreased levels of fructose-bisphosphatase 1 (FBP1) and phosphoglycerate kinase 1 (PGK1) were observed in DSCs compared to that in ESCs. FBP is an endogenous intermediate of the glycolytic pathway that is produced by PFK1 activity, through phosphorylation of fructose 6-phosphate (F6P), and removed by FBP1 activity (17). As shown in Fig. 1, with increased PFK1 and decreased FBP1 levels, the FBP level in DSCs was significantly increased compared to that in ESCs (Fig. 1, A to D). Compared to nonpregnant women, large amounts of FBP were found in the plasma and decidualized endometrium from women with normal pregnancy (Fig. 1E). Therefore, FBP accumulation could be associated with the change in PFK1/FBP1 levels during decidualization (Fig. 1F). Exposure to estrogen plus progesterone, or the supernatant of primary trophoblast cells significantly decreased FBP1 and elevated PFK1 in ESCs (Fig. 1, G and H), along with high levels of FBP and 3-phosphoglyceride (3-PGA) (fig. S1). In addition, the treatment with trophoblast supernatant led to the elevation of the levels of F6P and glyceraldehyde-3-phosphate (3-GAP) (fig. S1). These data indicate that endocrine environment and trophoblasts derived from the embryo likely play a role in the enrichment of FBP in DSCs during decidualization in early pregnancy.

Abnormal FBP–IL-27 regulatory axis in DSCs leads to pregnancy loss

To explore the possible relationship between FBP accumulation and normal pregnancy, pregnant mice were treated with or without 2-deoxy-D-glucose (2-DG), a glucose analog with dual activity of inhibiting glycolysis. Compared to the normal embryo group, FBP level was significantly decreased in the uterus of the embryo absorption group, especially in the 2-DG-treated pregnant mice (Fig. 2A). Constantly, expression of FBP1 was increased and that of PFK1 was decreased in the uteri of the embryo absorption group as compared to the control group (fig. S2). Exposure to 2-DG significantly increased embryo loss rates in mice (Fig. 2, B and C) but did not influence embryo growth significantly (Fig. 2D). FBP supplementation prevented embryo loss induced by 2-DG in vivo (Fig. 2, B and C). The results suggest that the absence of FBP in decidua contributes to embryo loss.

To investigate the possible mechanism underlying the absence of FBP in DSCs leading to embryo loss, a proteomic microarray was performed to evaluate the differential proteins of supernatants between control ESCs and FBP-treated ESCs; the differential expression of cytokines (differential fold > 3) was presented in Fig. 3A. Further analysis showed that both FBP and progesterone elevated interleukin-27 (IL-27) expression (Fig. 3, B and C); however, FBP1 overexpression (FBP1^{over}) decreased IL-27 expression in ESCs (Fig. 3C). We observed that the expression of IL-27 was significantly increased during decidualization, especially in DSCs (Fig. 3D). Consistent with the in vitro data, FBP administration significantly increased IL-27 levels in 2-DG-treated pregnant mice (fig. S3).

IL-27 receptor (IL-27R) is a heterodimer composed of the orphan cytokine receptor IL-27RA and the signal-transducing chain glycoprotein 130 (gp130) (18). IL-27RA is unique to IL-27R, whereas the gp130 subunit is shared with receptors for IL-6 and IL-35. Notably, increased embryo loss and restricted growth of embryos were observed in the *Il27ra* knockout (*Il27ra*^{-/-}) pregnant mice (Fig. 3, E to G). The levels of decidualization-related molecules, including *bone morphogenetic protein 2* (*Bmp2*), *Wnt4*, *Hoxa10*, *Cebpb*, *Dprp*, *insulin-like growth factor-binding protein 1* (*Igfbp1*), *Ihh*, *Il11*, *prolactin receptor* (*Prlr*), and *leukemia inhibitory factor* (*Lif*), were obviously decreased in the uterus of *Il27ra*^{-/-} pregnant mice (Fig. 3H), along with the depth of trophoblast infiltration into the uterus (Fig. 3I). The data together suggest that the abnormal FBP–IL-27 regulatory axis of DSC increases the risk of pregnancy loss.

A PKM2/ERK1/2/c-FOS pathway is involved in the regulation of IL-27 in DSCs by FBP

FOS participates in the formation of transcription factor complex AP-1, which is an important regulator of *IL27* (19). Further analysis showed that FBP significantly activated extracellular signal-regulated kinase 1/2 (ERK1/2) and c-FOS (Fig. 4, A and B), and the effects could be reversed by the inhibitor of ERK1/2 (fig. S4). In addition, the inhibitor of the ERK1/2 or c-FOS signaling suppressed IL-27 secretion in ESCs induced by FBP (Fig. 4C), suggesting that the stimulatory effect of FBP on IL-27 secretion in ESCs is dependent on the activation of ERK1/2 and c-fos signaling pathways.

To explore the possible mechanism of FBP on the ERK1/2/c-fos/IL-27 signaling, biotin-conjugated FBP (FBP-Biotin) and biotin-conjugated glucose-6-phosphate (G6P) (G6P-Biotin) were chemically synthesized, and the HuProt 20K protein array was performed to analyze the sense proteins of FBP in ESCs. As shown, 69 proteins were bound to FBP rather than to G6P (Fig. 4D). On the basis of the STRING database, we obtained the protein-protein interaction (PPI) network across the 69 proteins, FOS, mitogen-activated protein kinase 1 (MAPK1), and IL-27 (Fig. 4E). Among the related molecules in the PPI network, pyruvate kinase 2 (PKM2) was the core molecule for interaction with MAPK and FOS. As shown, activation of PKM2 by mitapivat up-regulated the phosphorylation of ERK1/2 and c-fos and the secretion of IL-27 in ESCs (Fig. 4, F to H). The addition of 2-DG led to the dephosphorylation of ERK1/2 and c-fos in vivo, and the decrease of IL-27 levels in the uterus of pregnant mice (Fig. 4, F to H). The results reveal that the PKM2/ERK1/2/c-FOS pathway plays an important role in FBP regulation of IL-27 expression in DSCs.

IL-27 maintains normal pregnancy by inducing decidual COX-2⁺ macrophage differentiation

To analyze the potential mechanisms of the FBP–IL-27 axis in the decidua during pregnancy, expressions of IL-27RA and gp130 at the maternal-fetal interface were explored. Compared to DSCs and trophoblast, decidual leukocytes (DLCs), especially dMφs, had higher levels of IL-27Rs (Fig. 5, A and B). Further analysis showed that either FBP-treated ESCs or IL-27^{over} ESCs promoted the phosphorylation of signal transducer and activator of transcription 3 (STAT3) in dMφ in vitro (Fig. 5, C and D). Positive feedbacks between STAT3 and cyclooxygenase-2 (COX-2)/prostaglandin E₂ (PGE₂) have been reported in various cancer cells and noncancer cells (20, 21). COX-2 was also highly expressed in CD45⁺CD14⁺ dMφs (Fig. 5, E and F). FBP-pretreated ESCs significantly increased

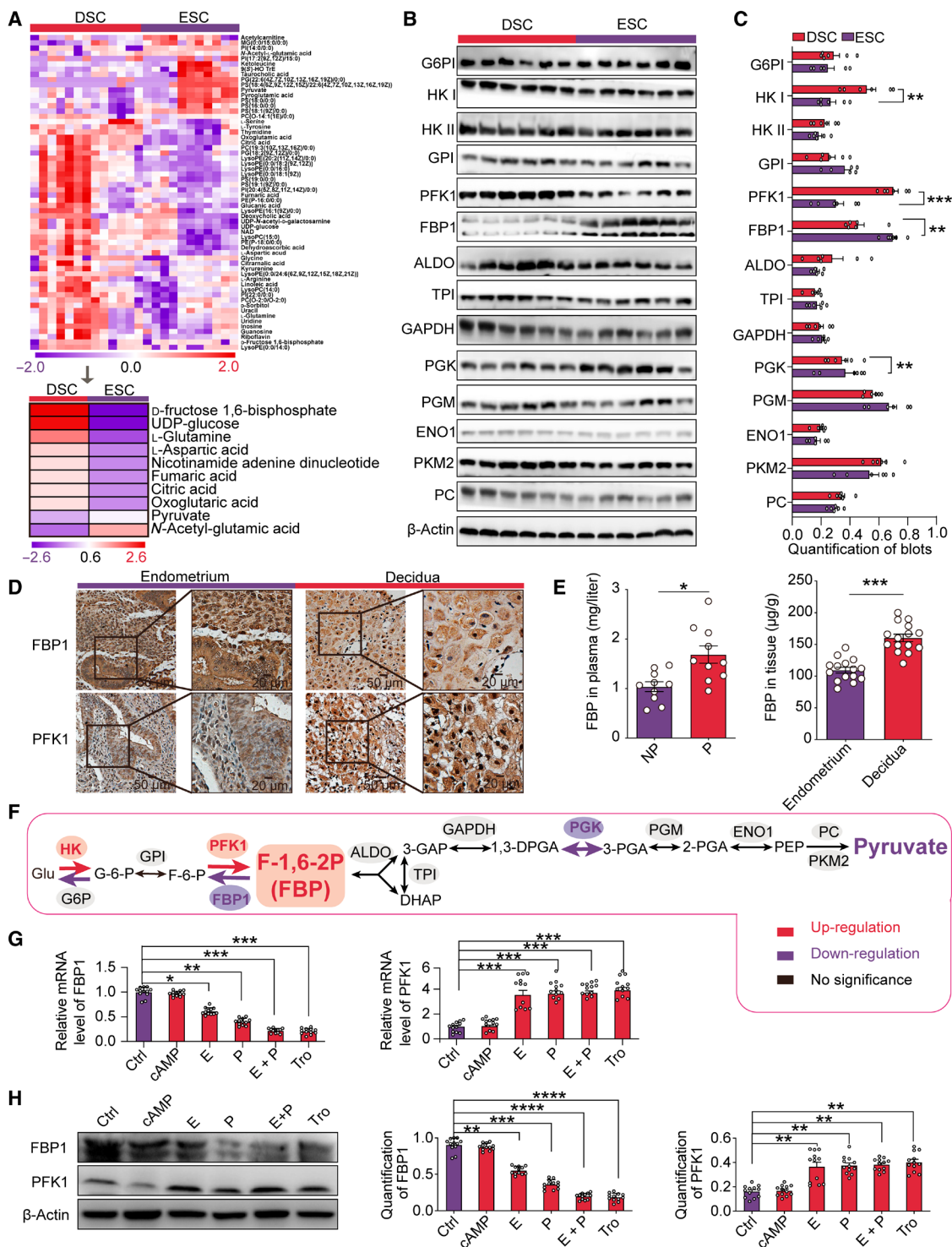


Fig. 1. FBP is enriched during decidualization. (A) Heatmap of differential metabolites in ESCs ($n = 12$) from healthy control endometrium of secretory phase and DSCs ($n = 12$) from normal early pregnant women by metabolomics analysis and list of differential metabolites in glycol metabolism. (B and C) Expression of metabolic enzymes of glycol metabolism between ESCs ($n = 6$) and DSCs ($n = 6$) was detected by Western blotting. (D) Expression of FBP1 and PFK1 between control endometrium ($n = 6$) and decidua tissues ($n = 6$) was detected by immunohistochemistry. (E) The FBP levels in blood plasma from women without (NP; $n = 10$) or with pregnancy (P; $n = 10$) and in endometrium ($n = 15$) or decidua tissues ($n = 15$) were detected with the FBP kits. (F) Summary of glycolysis characteristics during decidualization. (G and H) FBP1 and PFK1 levels in ESCs ($n = 12$) were detected by RT-PCR and Western blotting after pretreatment with 1% DMSO (Ctrl), adenosine 3',5'-monophosphate (cAMP; $0.5 \mu\text{M}$), and estrogen (E; $10^{-8} \mu\text{M}$) or plus progesterone (P; $10^{-6} \mu\text{M}$) or indirectly cocultured with primary trophoblast cells (Tro; ratio 1:1, 48 hours). Data were presented as means \pm SEM and analyzed by t test or one-way ANOVA test. * $P < 0.05$, ** $P < 0.01$, *** $P < 0.001$, and **** $P < 0.0001$.

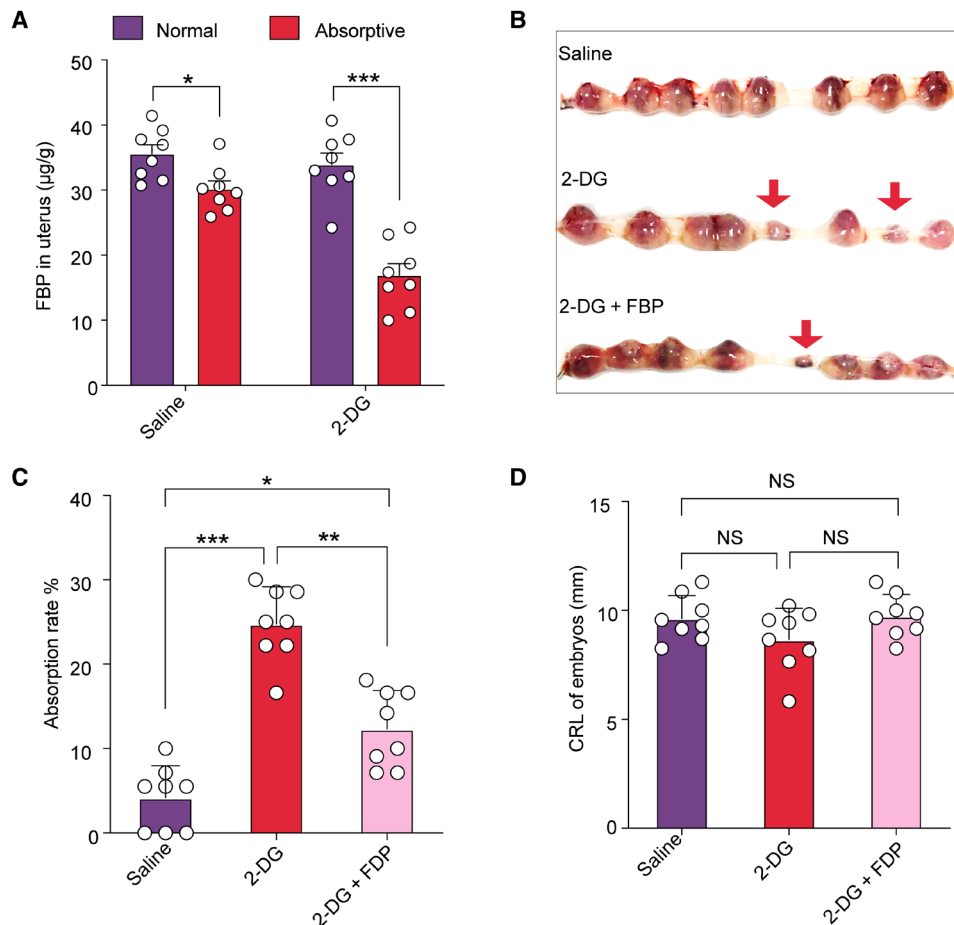


Fig. 2. FBP relieves 2-DG-mediated pregnancy loss. (A) The FBP levels in uterine tissues of pregnant mice treated with saline (1%, $n=8$) or 2-DG (50 mg/kg per day, $n=8$) were detected with FBP kits. (B to D) Photograph (red arrow: absorption point) of uterus from pregnant mice intraperitoneally injected with 1% saline ($n=8$), 2-DG (50 mg/kg per day, $n=8$), or 2-DG (50 mg/kg per day) plus FBP (500 mg/kg per day) ($n=8$). The absorption rates or crown-rump length (CRL) of embryos from (B) were analyzed in (C) or (D), respectively. Data were presented as means \pm SEM and analyzed by t test or one-way ANOVA test. * $P < 0.05$, ** $P < 0.01$, and *** $P < 0.001$; NS, no significance.

COX-2 levels in dMφs (Fig. 5G), and coculture with ESCs, especially IL-27^{over} ESCs, resulted in an increase of COX-2 levels in dMφs, (Fig. 5H). However, COX-2 levels were low in the uterus of *Il27ra*^{-/-} pregnant mice (Fig. 6A).

Macrophage polarization has been reported to play an important role in normal pregnancy (13, 22). Compared to COX-2⁻ dMφs, COX-2⁺ dMφs exhibited higher levels of CD163, CD206, CD209, and indolamine 2,3-dioxygenase 1 (IDO1) and lower levels of interferon- γ (IFN- γ), IL-23, and interferon regulatory factor 4 (IRF4) (fig. S5A), suggesting that COX-2⁺ dMφs present an M2-like phenotype. In addition, FBP-pretreated ESCs and IL-27^{over} ESCs promoted M2-like differentiation of dMφs in the coculture system (fig. S5B). 2-DG decreased COX-2⁺ macrophage levels in the uterus of pregnant mice in vivo (Fig. 6B). Intraperitoneal injection of celecoxib (a COX-2-specific inhibitor) led to the decrease of M2-like macrophage in mouse uterus and an increase of pregnancy loss rates (fig. S6). Similarly, *Ptgs2* (COX-2)^{-/-} mice presented fewer M2-like macrophage in mouse uterus, with impairment of decidualization, abnormal placental development, and size-reduced embryos; these female mice were further prone to embryo loss or IUGR (Fig. 6, C to F, and fig. S7). Overall, the results indicate that FBP-IL-27 triggers COX-2⁺ M2-like Mφ differentiation during decidualization and maintains normal pregnancy.

To further analyze the possible mechanism of IL-27RA dMφs and COX-2⁺ dMφs in the maintenance of normal pregnancy, differential proteins in the supernatants between IL-27RA⁺ dMφ and IL-27RA⁻ dMφ were evaluated by a proteomic microarray (fig. S8A). Detailed analysis showed that 9 differential proteins were associated with decidualization, and 24 differential proteins were involved in trophoblast invasion (Fig. 6G and fig. S8B). The findings were further validated via adoptive transfer of macrophages, which could be detected in the uterus of pregnant mice (fig. S9). Contrary to that of COX-2⁻ macrophages from *Ptgs2*^{-/-} pregnant mice, adoptive transfer of macrophages from wild-type (WT) mice restored decidualization and the depth of trophoblast infiltration and decreased the risk of pregnancy loss (Fig. 6, H to J) in *Il27ra*^{-/-} pregnant mice. The data suggest that COX-2⁺ dMφs prevent pregnancy loss induced by the absence of the IL-27/IL-27RA signal axis by promoting decidualization and trophoblast invasion.

FBP administration induces COX-2⁺ dMφ differentiation and further alleviates pregnancy loss

To determine the profile of the FBP-IL-27-COX-2⁺ dMφ axis in patients, both decidua and plasma were collected from patients experiencing unexplained recurrent spontaneous abortion (RSA).

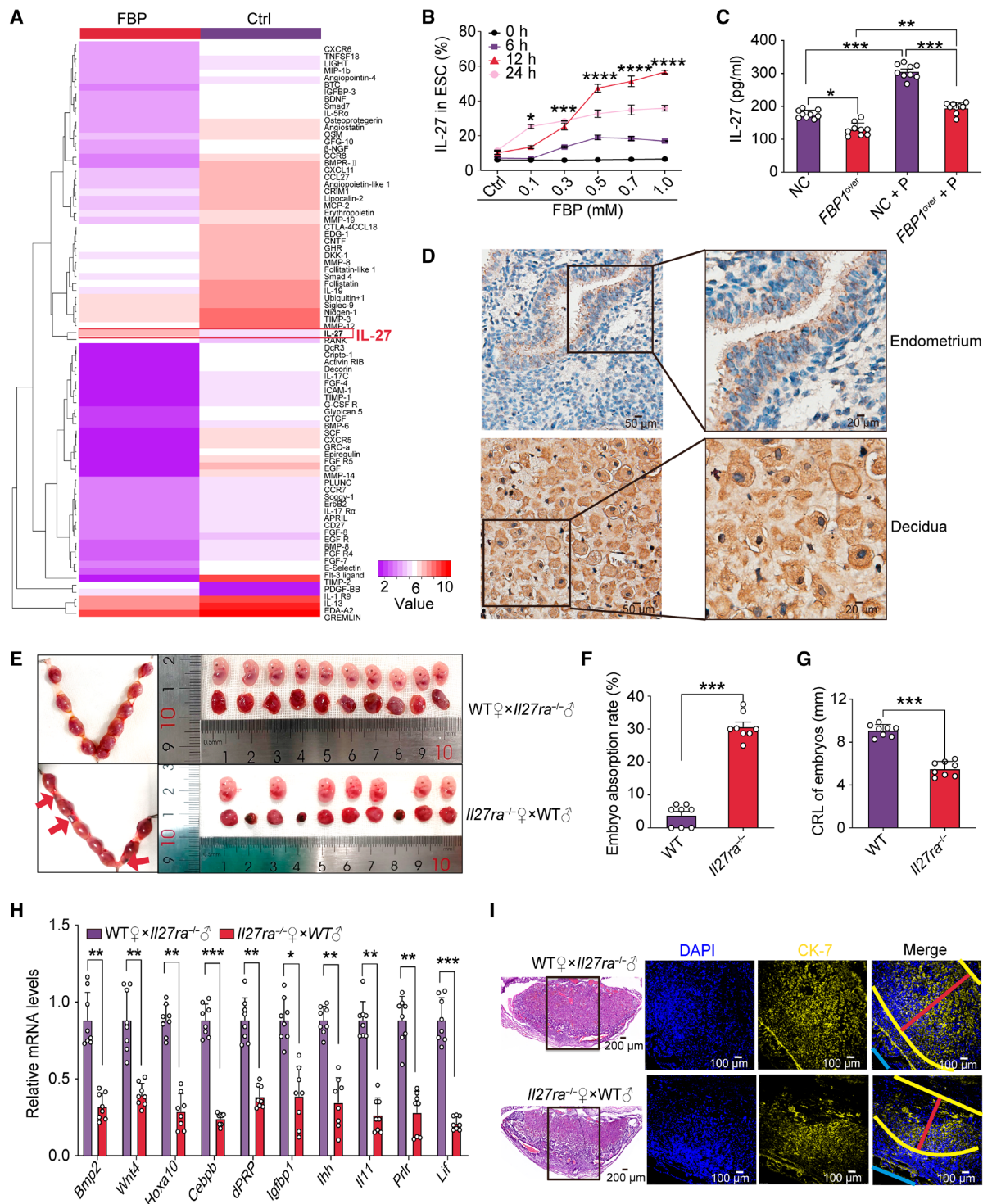


Fig. 3. Abnormal FBP-IL-27 regulatory axis in DSCs leads to pregnancy loss. (A) Heatmap of the differential proteins (differential fold > 3) of supernatants between FBP (0.5 mM)–ESC ($n = 3$) and Ctrl-ESC ($n = 3$) by the proteomic microarray. **(B)** The IL-27 levels in ESCs ($n = 9$) treated with FBP were detected by FCM. **(C)** The IL-27 levels in supernatants of control ESCs (*FBP1*-NC, $n = 9$) or *FBP1*-overexpressing ESCs (*FBP1*^{over}, $n = 9$) treated with DMSO (1%) or progesterone (P; 10⁻⁸ μ M) were detected by ELISA. **(D)** Expression of IL-27 between control endometrium ($n = 6$) and decidua tissues ($n = 6$) was detected by immunohistochemistry. **(E to G)** Photograph (red arrow: absorption point) of uterus, absorption rates, or CRL of embryos from WT pregnant mice (mated with male *Il27ra*^{-/-} mice, $n = 8$) or *Il27ra*^{-/-} pregnant mice (mated with male WT mice, $n = 8$). **(H)** Transcription levels of decidualization-related genes in uterus from (E) were analyzed by RT-PCR. **(I)** Depth of CK7⁺ trophoblast infiltration into uterus from (E) was observed by hematoxylin and eosin staining or immunofluorescence assays. DAPI, 4',6-diamidino-2-phenylindole. Data were presented as means \pm SEM and analyzed by *t* test or one-way ANOVA test. * $P < 0.05$, ** $P < 0.01$, *** $P < 0.001$, and **** $P < 0.0001$.

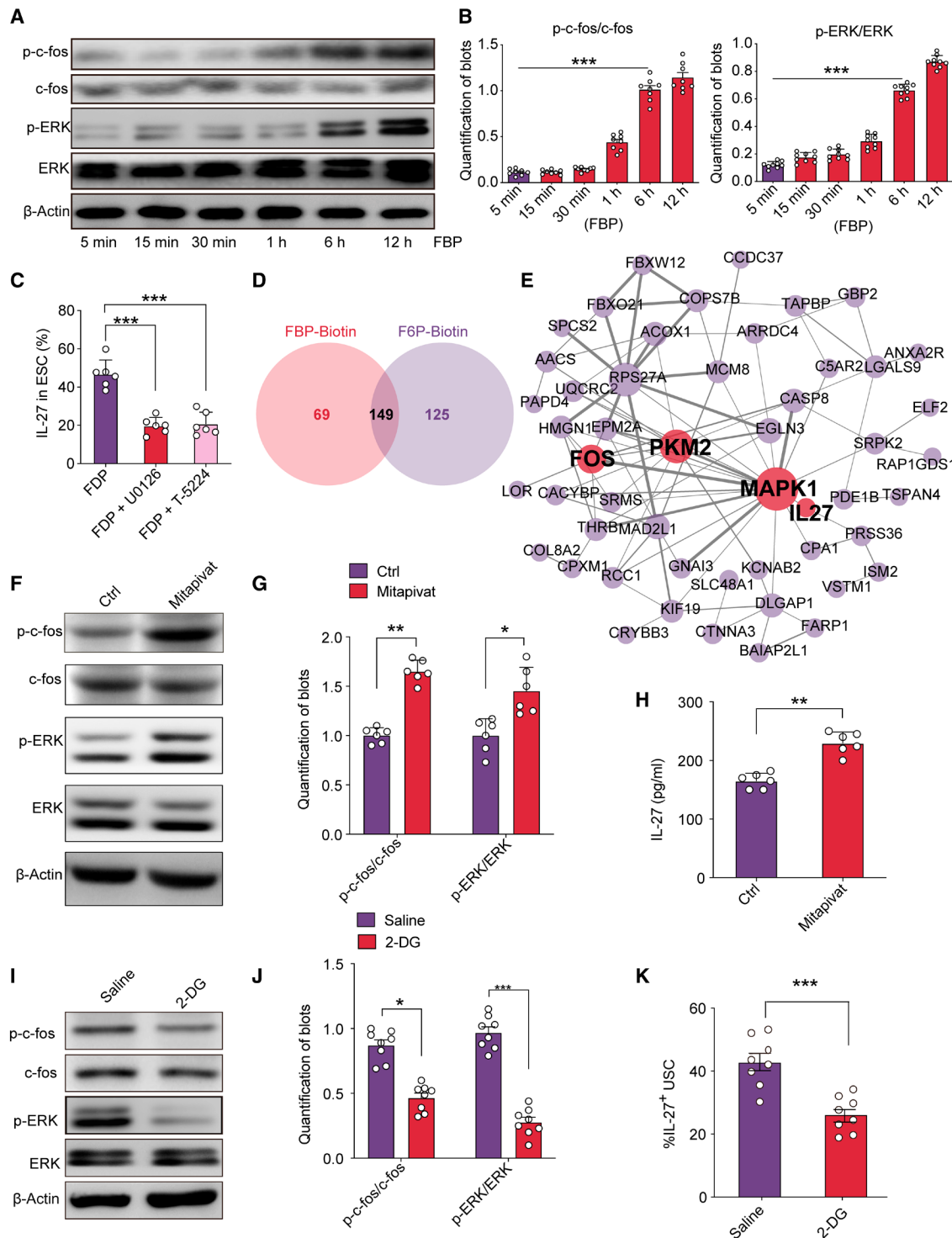


Fig. 4. FBP increases IL-27 expression in DSCs in a PKM2/ERK1/2/c-FOS–dependent manner. (A and B) Expression of p-c-fos, c-fos, p-ERK, or ERK in FBP (0.5 mM)–treated ESCs ($n = 9$) was analyzed by Western blotting. (C) The IL-27 levels in supernatants of FBP, FBP, and ERK1/2 inhibitor (U0126, 10 μ M) or FBP and c-fos inhibitor (T-5224, 20 mM)–treated ESCs (24 hours, $n = 6$) were detected by ELISA. (D) Sense proteins of FBP and G6P in ESCs were analyzed by the HuProt 20K protein array. (E) PPI network based on the STRING database between 69 proteins from (D), FOS, MAPK1, and IL27. (F to H) The expression of p-c-fos, c-fos, p-ERK, or ERK and secretion levels of IL-27 in a PKM2 activator (mitapivat, 10 μ M) or DMSO (Ctrl, 1%)–treated ESCs (24 hours, $n = 6$) were analyzed by Western blotting and ELISA. (I to K) Expression of p-c-fos, c-fos, p-ERK, or ERK in uterus and IL-27 levels in USCs from pregnant mice ($n = 8$) treated with saline (1%) or 2-DG (50 mg/kg per day) were analyzed by Western blotting and ELISA. Data were presented as means \pm SEM and analyzed by t test or one-way ANOVA test. * $P < 0.05$, ** $P < 0.01$, and *** $P < 0.001$.

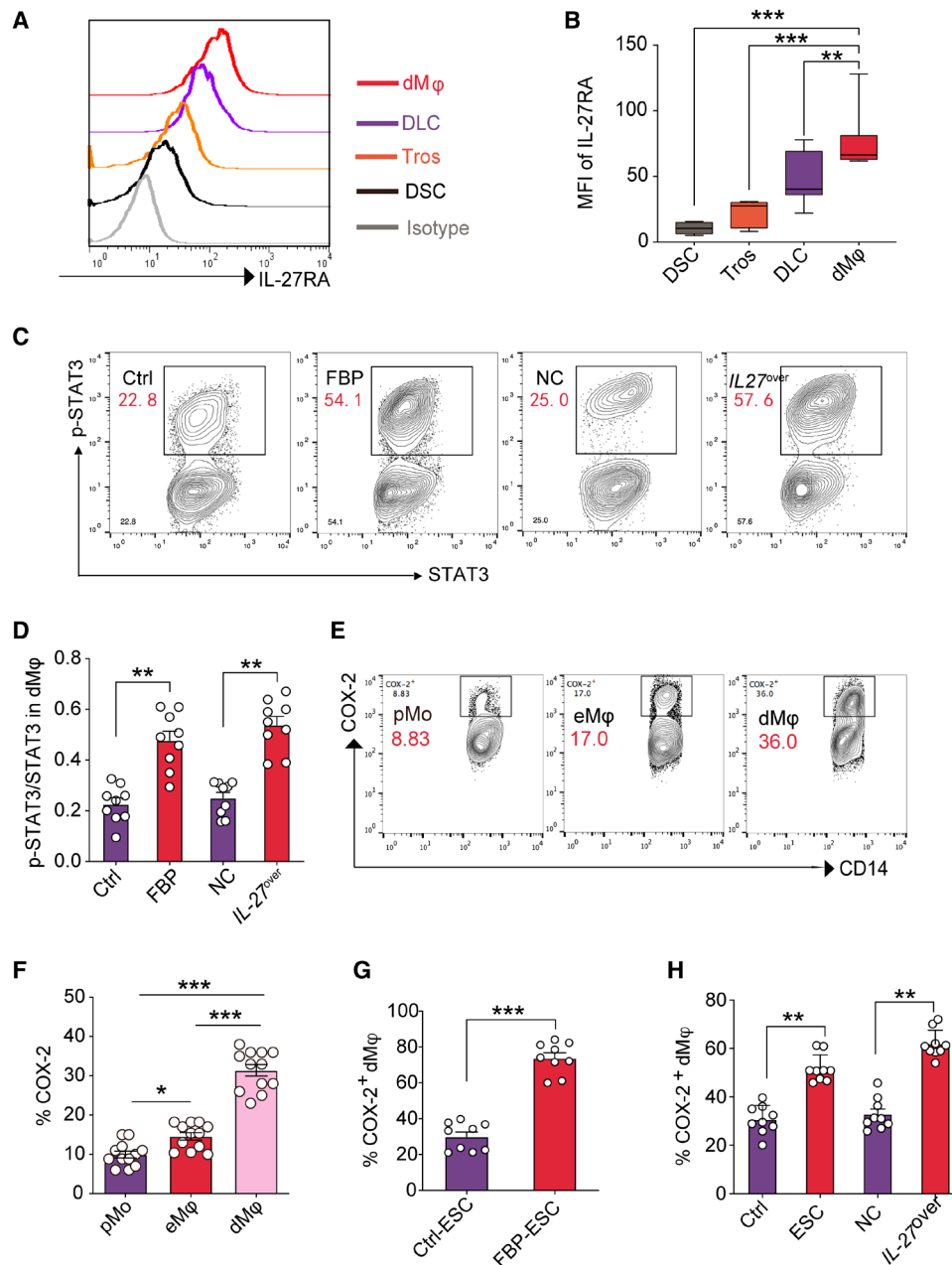


Fig. 5. IL-27 induces decidual COX-2⁺ macrophage differentiation in vitro. (A and B) Expression of IL-27RA in DSCs ($n = 9$), trophoblast cells (Tros; $n = 9$), DLCs ($n = 9$), and decidual macrophages (dMφs) ($n = 9$) was analyzed by FCM. Statistical graph of (A) was shown in (B). (C and D) Expression of p-STAT3 and STAT3 in dMφs ($n = 9$) after coculture with ESCs pretreated with FBP (0.5 mM for 24 hours) or transfected with *IL-27* overexpression plasmids (*IL-27^{over}*) for 48 hours was detected by FCM, and the ratios of p-STAT3 to STAT3 were calculated. (E and F) Expression of COX-2 in peripheral blood monocytes (pMos) ($n = 12$), eMφs ($n = 12$), and dMφs ($n = 12$) was analyzed by FCM. Statistical graph of (E) was shown in (F). (G) Expression of COX-2 in dMφs ($n = 9$) cocultured with Ctrl or FBP (0.5 mM for 24 hours)-treated ESCs was detected by FCM. (H) Expression of COX-2 in dMφs ($n = 9$) cocultured with FBP (0.5 mM for 24 hours)-pretreated ESCs or *IL-27^{over}* ESCs for 48 hours was detected by FCM. Data were presented as means \pm SEM or median and quartile and analyzed by *t* test, one-way ANOVA test, or Kruskal-Wallis test. * $P < 0.05$, ** $P < 0.01$, and *** $P < 0.001$.

As shown, DSCs from patients with unexplained RSA exhibited a significant decrease of PFK1, along with an increase of FBP1 levels (Fig. 7, A to C). Low levels of FBP in plasma and decidua were observed in patients with RSA (Fig. 7D), and the differences were not observed between the plasma of nonpregnant patients and healthy pregnant women (Fig. 7D). Reverse transcription polymerase chain reaction (RT-PCR) and immunohistochemical analysis showed lower levels

of IL-27 in DSCs from patients with RSA (Fig. 7, E to G), as well as a lower percentage of COX-2⁺ M2-like dMφs (Fig. 7, H and I). The results indicate that patients with unexplained RSA display insufficient FBP-IL-27 expression and COX-2⁺ Mφ in the decidua.

In CBA/J \times DBA/2 matings [a spontaneous abortion-prone model (SA)], a significant absence of FBP was observed in the uterus compared to that in CBA/J \times BALB/c matings (a mouse model of normal

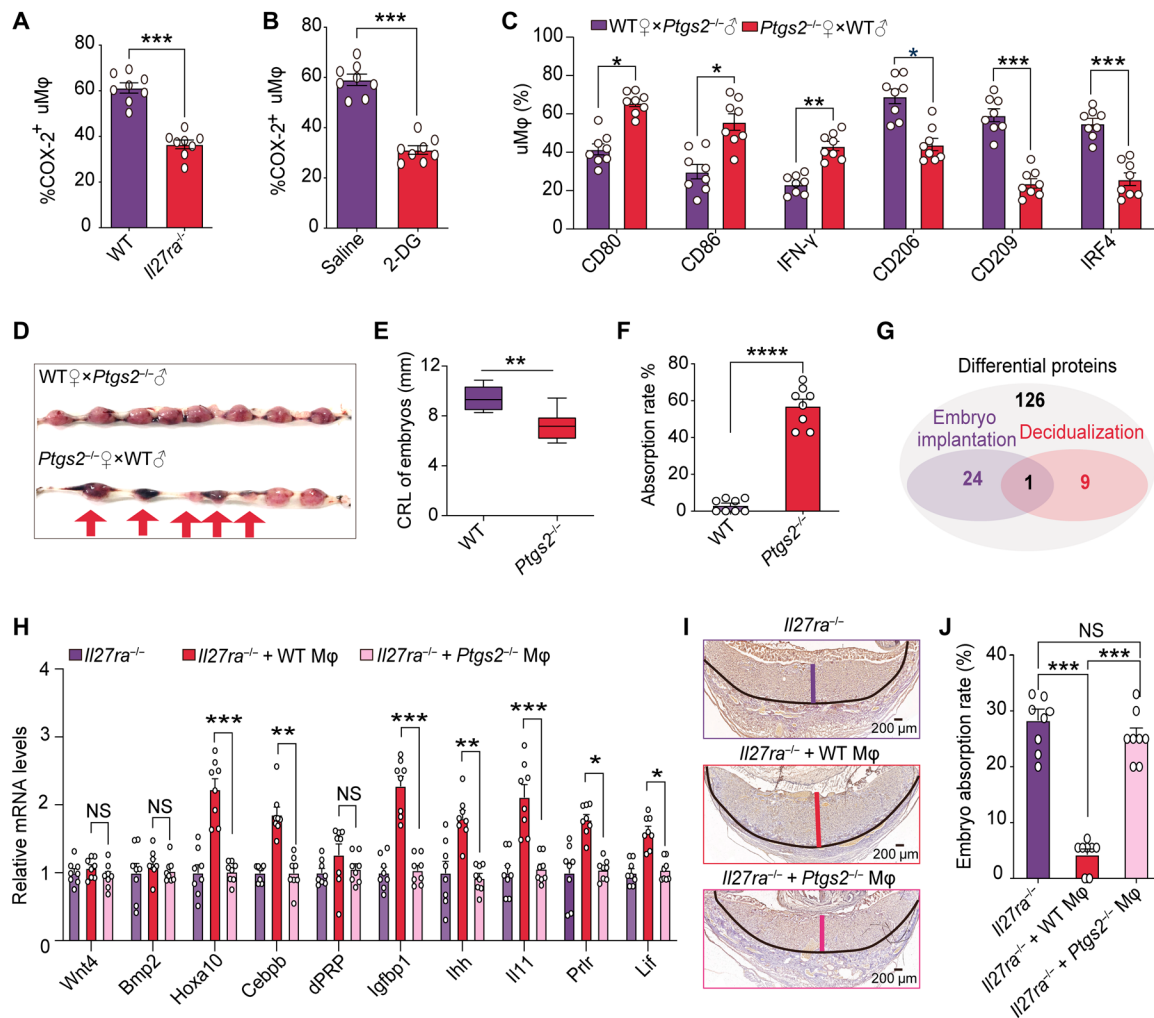


Fig. 6. IL-27 maintains normal pregnancy in a uterine COX-2⁺ macrophage-dependent manner. (A) Expression of COX-2 in uMφs of WT (mated with male *Il27ra*^{-/-} mice, *n* = 8) or *Il27ra*^{-/-} pregnant mice (mated with male WT mice, *n* = 8) was detected by FCM. (B) Expression of COX-2 in uMφs of saline (1%, *n* = 8) or 2-DG (50 mg/kg per day, *n* = 8)-treated pregnant mice was detected by FCM. (C) Expression of differentiation molecules in uMφs of WT (*n* = 8) or *Ptg2*^{-/-} pregnant mice (*n* = 8) was detected by FCM. (D to F) Photograph (red arrow: absorption point) of uterus, the CRL of embryos, or absorption rates from WT (*n* = 8) or *Ptg2*^{-/-} pregnant mice (*n* = 8). (G) Differential proteins of supernatants between IL-27RA⁺ dMφs and IL-27RA⁻ dMφs were evaluated by the proteomic microarray. (H to J) Transcription levels of decidualization-related genes in uterus, depth of CK7⁺ trophoblast infiltration into uterus, and embryo absorption rates of *Il27ra*^{-/-} pregnant mice (mated with male WT mice, *n* = 8) adopted with WT or *Ptg2*^{-/-} macrophages. Data were presented as means ± SEM or median and quartile and analyzed by *t* test, Mann-Whitney *U* test, or one-way ANOVA test. **P* < 0.05, ***P* < 0.01, and ****P* < 0.001.

pregnancy) (Fig. 8A). Intraperitoneal injection of FBP led to the increase of FBP levels in both uterus and plasma of SA mice (Fig. 8, A and B). FBP also elevated IL-27 expression in uterine stromal cells (USCs) of SA mice (Fig. 8, C and D), along with a high percentage of COX-2⁺ M2-like macrophages, regulatory T cells, and T helper 2 (T_H2) bias (Fig. 8, E and F, and fig. S10). Supplementation with FBP promoted decidualization (Fig. 8G) and trophoblast invasion (Fig. 8H) and prevented pregnancy loss (Fig. 8, I and J) in SA mice. Together, the data suggest that supplementation with FBP decreases the risk of pregnancy loss due to insufficient FBP–IL-27 expression and COX-2⁺ dMφs.

DISCUSSION

Decidualization, a process where extensive remodeling of the endometrium occurs to create a receptive environment for embryonic

development, is a key event in pregnancy in some mammals including mice and humans. Glucose is required for both embryonic development and decidualization of the endometrium (23). Glucose is metabolized via multiple pathways in the murine uterus to support decidualization and provide adenosine triphosphate (ATP) (24). Inhibition of glucose metabolism impairs decidualization in mice, resulting in smaller litters (25, 26). However, the features and effects of glucose metabolism during decidualization in humans are mostly unknown. With increased PFK1 and decreased FBP1 levels reported here, accumulation of FBP was realized in decidualized human stromal cells. In addition, exposure to progesterone plus estrogen, or trophoblast supernatant, led to the increase of PFK1 and decrease of FBP1 levels in vitro. The phosphatidylinositol 3-kinase (PI3K)/AKT-dependent PFK1 activation and glucose transporter type 1 (GLUT1) expression had previously been shown to promote

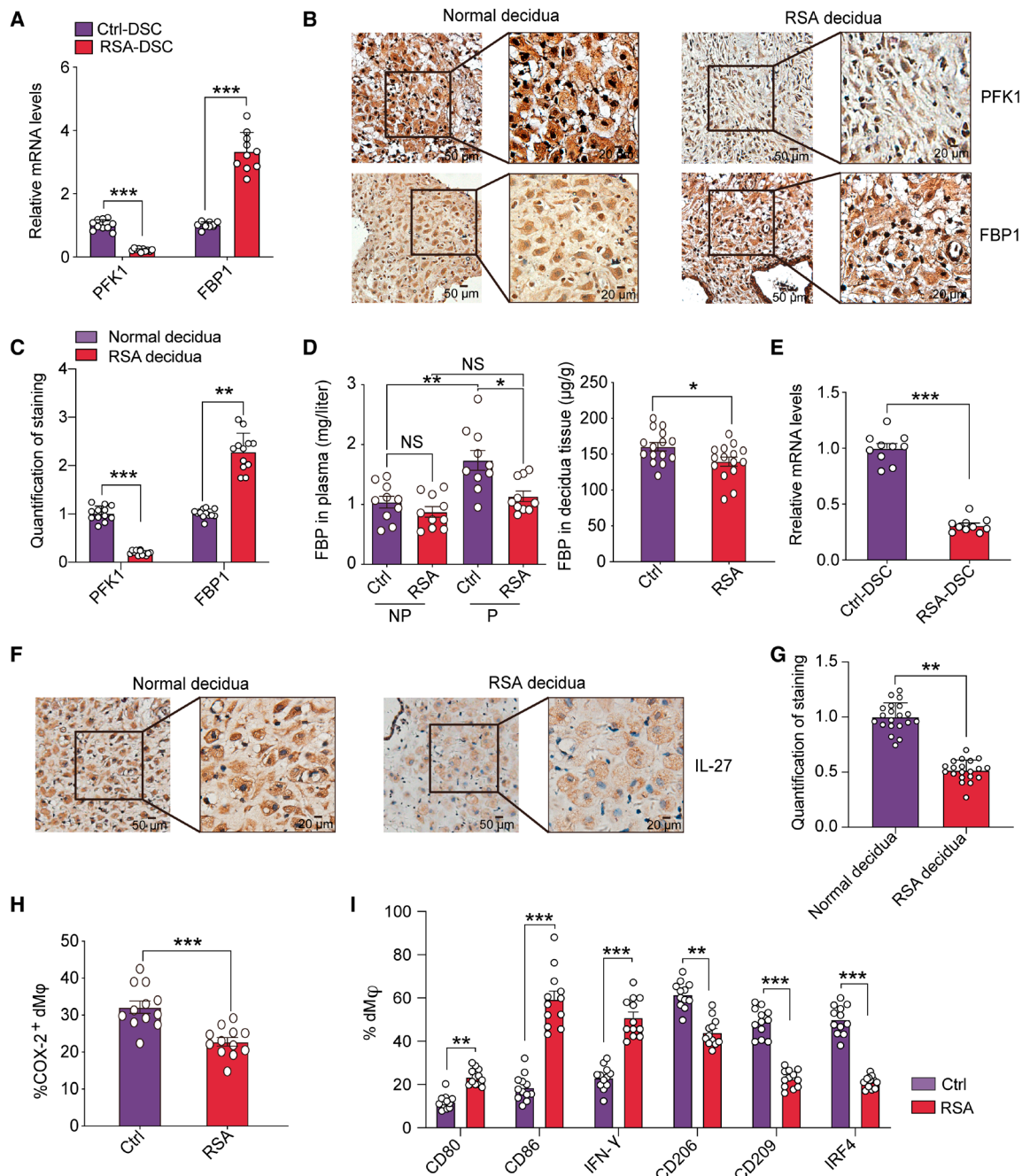


Fig. 7. The FBP-IL-27-COX-2 regulatory axis in decidua is insufficient in patients with unexplained RSA. (A) The mRNA levels of FBP1 and PFK1 between DSCs from normal pregnant women ($n = 10$) or patients with unexplained RSA ($n = 10$) were detected by RT-PCR. (B and C) Expression of FBP1 and PFK1 between decidua tissues from normal pregnant women ($n = 12$) or patients with unexplained RSA ($n = 12$) were detected by immunohistochemistry. (D) The FBP levels in the blood plasma from nonpregnant (NP) or pregnant (P) normal women or patients with unexplained RSA ($n = 10$ per group) were detected. (E) The mRNA level of IL-27 between DSCs from normal pregnant women ($n = 10$) or patients with unexplained RSA ($n = 10$) was detected by RT-PCR. (F and G) Expression of IL-27 between decidua tissues from normal pregnant women ($n = 20$) or patients with unexplained RSA ($n = 20$) was detected by immunohistochemistry. (H and I) The levels of COX-2 (H), CD80, CD86, INF- γ , CD206, CD209, and IRF4 (I) in dMfps from normal pregnant women ($n = 12$) or patients with unexplained RSA ($n = 12$) were detected by FCM. Data were presented as means \pm SEM and analyzed by t test or one-way ANOVA test. * $P < 0.05$, ** $P < 0.01$, and *** $P < 0.001$.

the production of FBP and the Warburg effect (17), and progesterone was reported to activate hypoxia-inducible factor 1 α and c-Myc in vitro, through PI3K/AKT signaling pathway to maintain aerobic glycolysis in decidualizing cells (24). The data suggest that decidualization induced by pregnancy-related hormones and trophoblast

supernatant promotes the enrichment of FBP possibly by PI3K/AKT-dependent PFK1 activation and glucose uptake. As a high-energy endogenous intermediate of the glycolytic pathway, FBP is considered responsible for sustaining glycolysis and increasing ATP production, eventually accelerating the decidualization, and

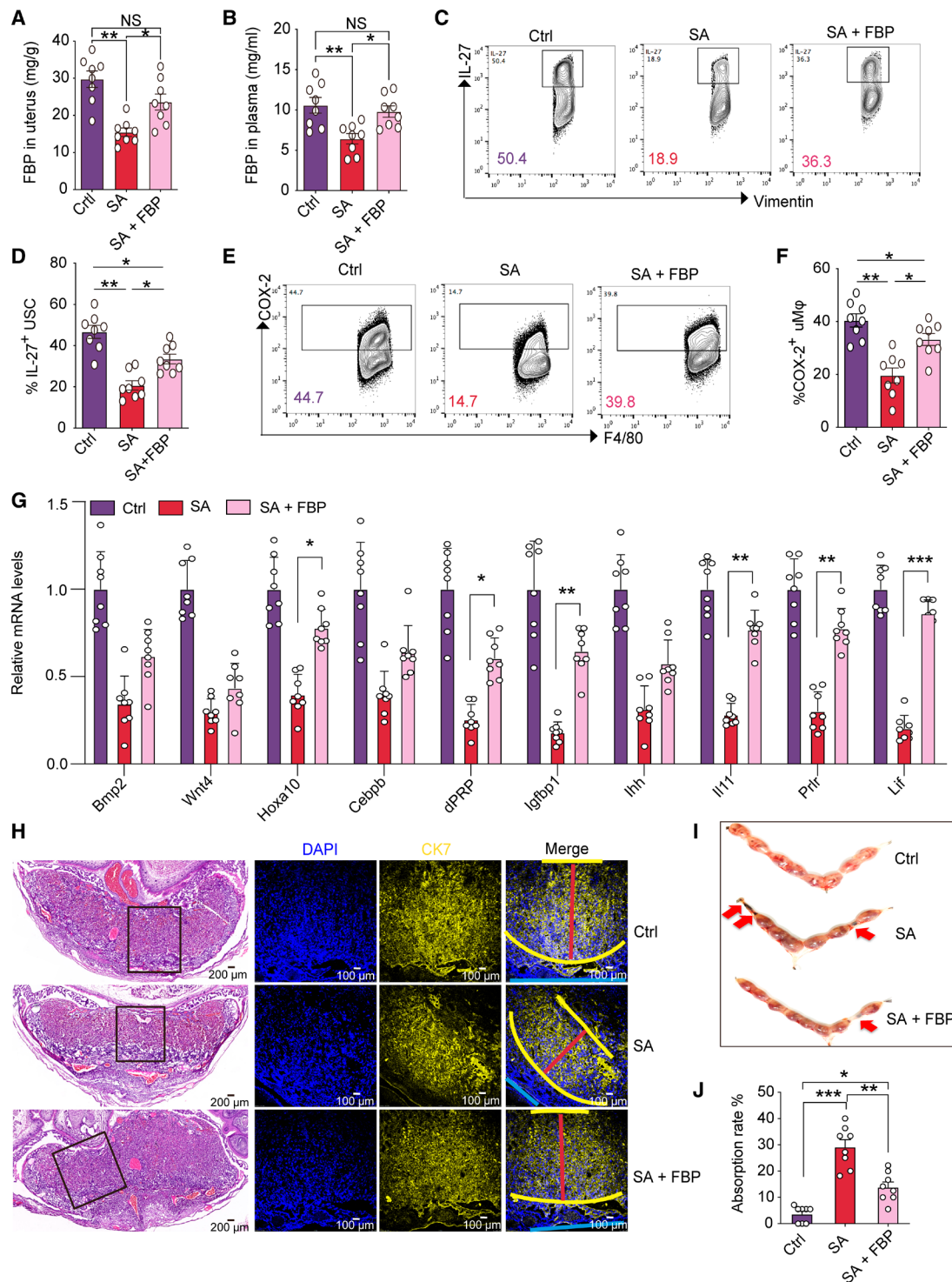


Fig. 8. FBP administration induces COX-2⁺ dMφ differentiation and alleviates pregnancy loss. (A and B) The FBP levels in uterine tissues and blood plasma of normal pregnant mice (Ctrl, *n* = 8), spontaneous abortion-prone mice (SA; *n* = 8), or SA mice intraperitoneally injected with FBP (500 mg/kg per day, SA + FBP, *n* = 8) were detected. (C and D) The IL-27 levels in USCs of pregnant mice from Ctrl (*n* = 8), SA (*n* = 8), or SA + FBP (*n* = 8) group were analyzed by FCM. (E and F) The COX-2 levels in uMφ of pregnant mice from Ctrl (*n* = 8), SA (*n* = 8), or SA + FBP (*n* = 8) group were analyzed by FCM. (G) The mRNA levels of decidualization-related genes in uterus of pregnant mice from Ctrl (*n* = 8), SA (*n* = 8), or SA + FBP (*n* = 8) group were detected by RT-PCR. (H) Depth of CK7⁺ trophoblast infiltration into uterus of pregnant mice from Ctrl (*n* = 8), SA (*n* = 8), or SA + FBP (*n* = 8) group was observed by hematoxylin and eosin staining or immunofluorescence staining. (I and J) Photograph (red arrow: absorption point) of uterus and absorption rates of pregnant mice from Ctrl (*n* = 8), SA (*n* = 8), or SA + FBP (*n* = 8) group. Data were presented as means ± SEM and analyzed by one-way ANOVA test. **P* < 0.05, ***P* < 0.01, and ****P* < 0.001.

further forming a positive feedback loop of decidualization–FBP enrichment–ATP production during early pregnancy.

Upon binding to PKM2, FBP induces higher production and secretion of IL-27 by ESC/DSC, which is achieved through the regulation of ERK and c-FOS signaling pathways. The ERK/c-FOS signaling is necessary for the successful decidualization and embryo implantation in mice as well as human ESCs (27, 28). Therefore, FBP (possibly by binding to the sensor protein PKM2) participates in decidualization by stimulating ATP production and activating the ERK/c-FOS signaling pathways. Previous studies have found that activation of PKM2 is responsible for the expression of genes that promote the Warburg effect in cancer cells, namely, *GLUT1* and lactate dehydrogenase A (*LDHA*) (29, 30). In accordance with the high levels of IL-27 in DSCs, we observed that FBP-PKM2 stimulated IL-27 production of ESC by activating the ERK/c-FOS signaling pathways together.

We found *Il27ra*^{-/-} pregnant mice to be prone to fetal loss or IUGR due to poor decidualization and reduced capacity of trophoblasts to invade the decidua. As a heterodimeric member of the IL-12 cytokine family, IL-27 induces IL-10-secreting type 1 regulatory (Tr1) cells, and Tim-3 and PD-L1 expression in CD4⁺ and CD8⁺ T cells (31, 32). IL-27RA and gp130 were highly expressed in the macrophages of human and mouse decidua. In addition, ESC/DSC-derived IL-27 promoted COX-2⁺ M2-like macrophage differentiation in decidua both in vitro and in vivo. Mechanistically, STAT3 activation should be involved in these processes. PGE₂ is an important regulator for M2 or M2-like macrophages in multiple physiological and pathological processes (33, 34). Therefore, the FBP–IL-27 axis–triggered M2-like macrophage in decidua should be due to the interaction between STAT3 and COX-2/PGE₂. However, the potential mechanism for this regulatory process at the maternal-fetal interface during early pregnancy needs further investigation.

Similar to *Il27ra*^{-/-} pregnant mice, *Ptgs2*^{-/-} females showed defective endometrial receptivity/decidualization and placentation, which was consistent with previous reports (35, 36). The process of decidualization is accompanied by the enrichment and redistribution of decidual immune cells. Disturbance of maternal-fetal immune regulation is associated with several complications of human pregnancy (e.g., miscarriage) (7, 37, 38). However, mechanisms underlying the metabolic reprogramming of immune cells during decidualization are almost unknown. Impaired M2-like macrophages were observed in the decidua of *Ptgs2*^{-/-} pregnant mice. Transfer of COX-2⁺ macrophages obviously prevented the impairment of decidualization, trophoblast invasion, and M2 macrophage differentiation in the uterus of *Il27ra*^{-/-} pregnant mice. The results indicate that the FBP–IL-27 axis–triggered COX-2⁺ M2-like macrophages in the decidua participate in the maintenance of maternal-fetal immune tolerance, decidualization, trophoblast invasion, and placenta development. However, whether COX-2–derived PGE₂ is involved in this regulatory process remains to be further clarified.

Exogenous administration of FBP has been shown to exert protective effects in a variety of ischemic injury diseases, which are attributed to the ability of FBP to sustain glycolysis and increase ATP production by serving as a high-energy substrate under pathological conditions (39–42). Targeting glycolysis with 2-DG also eliminated FBP enrichment and its downstream effects in the decidua, and jointly induced embryo loss. Moreover, we observed decreased levels of FBP in the decidua and plasma of patients with RSA. To the best of our knowledge, this is the first report of a

relationship between FBP and miscarriage. Detailed investigation showed that FBP supplementation–induced maternal-fetal immune tolerance promoted decidualization and placental development through IL-27–triggered COX-2⁺ M2-like macrophage and prevented pregnancy loss.

In conclusion, pregnancy-associated hormones, accompanied by implantation of the during normal pregnancy, trigger ESCs to differentiate into DSCs and further induce the enrichment of FBP (fig. S11). While FBP accelerates decidualization in an ATP-dependent manner, the FBP-PKM2 complex promotes the secretion of IL-27 by activating ERK1/2–c-FOS signaling pathways. Subsequently, IL-27 drives COX-2⁺ M2-like dMφ differentiation through STAT3 signaling. After differentiation is induced, these dMφs create and maintain a maternal-fetal tolerant microenvironment, along with promoting decidualization, trophoblast invasion, and placenta development. Once an imbalance in the FBP–IL-27–COX-2⁺ M2-like dMφ axis disturbs the interaction between DSCs and dMφs, pregnancy loss occurs. Supplementation with FBP can prevent pregnancy loss by activating the FBP–IL-27–COX-2⁺ M2-like dMφ axis. Therefore, our study suggests the potential uses of a metabolite, FBP, as an early-warning indicator of early pregnancy loss and as a possible therapeutic agent for its prevention.

MATERIALS AND METHODS

Patients and sample collection

The protocol for this study was approved by the Human Research Ethics Committee of Obstetrics and Gynecology Hospital, Fudan University, and written informed consent was obtained from all participants. First-trimester human peripheral blood was obtained from 60 women with clinically normal pregnancies [age, 29.78 ± 7.45 years; gestational age, 48.25 ± 6.7 days (mean ± SEM)], which were eventually terminated for nonmedical reasons, and from 33 women with RSA [age, 31.05 ± 7.31 years; gestational age at sampling, 48.17 ± 7.7 days (mean ± SEM)]. Peripheral blood (*n* = 22) and normal endometrial samples (*n* = 65) in the secretory phase were collected from 65 patients (age range, 30 to 45 years) who had undergone diagnostic curettage or hysterectomy for benign reasons unrelated to endometrial dysfunction as healthy controls. Decidual tissues were obtained from 144 women with clinically normal pregnancies [age, 29.10 ± 5.95 years; gestational age, 48.87 ± 6.61 days (mean ± SEM)] (terminated for nonmedical reasons) and from 47 women with RSA [age, 32.13 ± 7.19 years; gestational age, 52.41 ± 6.32 days (mean ± SD)]. All cases were histologically confirmed according to the established criteria. All pregnant women were confirmed by ultrasound and blood tests, and women with spontaneous miscarriage due to endocrine, anatomical, and genetic abnormalities, or due to any infection, were excluded.

Mice

Ptgs2 heterozygous mice were obtained from The Jackson Laboratory; *Ptgs2*^{-/-} and WT littermates were obtained by mating male and female heterozygous mice. *Il27ra*^{-/-} mice were bred by Shanghai Model Organisms Center Inc. (Shanghai, China), and all mice were maintained in the Laboratory Animal Facility of Fudan University (Shanghai, China). A group of adult female C57BL/6 mice were purchased from the Laboratory Animal Facility of Fudan University and used for this study. Female CBA/J, male DBA/2, and male BALB/c mice were all purchased from Beijing Huafukang Biotechnology Co. Ltd.

(China). After adaptive feeding, female CBA/J mice were mated with male BALB/c mice or male DBA/2 mice (2:1) to construct mouse models of normal pregnancy or of spontaneous abortion. They were usually maintained for 2 weeks in the animal facility before use. The Animal Care and Use Committee of Fudan University approved all animal protocols. Pregnant C57BL/6 mice were either injected intraperitoneally with 2-DG (50 mg/kg per day, order no. HY-13966, MedChemExpress LLC., Shanghai, China) plus FBP trisodium salt [500 mg/kg per day; order no. A600468 CAS (81028-91-3), Sangon Biotech (Shanghai) Co. Ltd., China] or not, or vehicle [1% dimethyl sulfoxide (DMSO), Sigma-Aldrich], from days 0 to 7 of pregnancy. The day of detection of vaginal hydrant was considered day 0 of gestation.

Immunostaining

Immunohistochemical staining was performed as described previously (43). Human endometrium and decidua were labeled with rabbit anti-human FBP1, PFK1, IL-27, and PKM antibodies (Abs) (dilution 1:100; sc-271241, sc-377346, sc-390482, and sc-365684, Santa Cruz Biotechnology); uterine tissues of pregnant mice were labeled with rabbit anti-mouse CK7 Abs (10 µg/ml; ab9021, Abcam) by immunohistochemical staining.

Metabolomics test (LC-MS analysis)

Human ESCs and DSCs were subjected to metabolomics tests. The cells were homogenized and lysed by sonication (30,000 Hz) in pre-chilled phosphate-buffered saline (PBS) buffer. Proteins in the supernatant were harvested after repeated centrifugation (1000g) with cold 85% acetone as metabolite-free proteome. Chromatography was performed using liquid chromatography–mass spectrometry (LC-MS) (Thermo Fisher Scientific, UltiMate 3000 LC, Orbitrap Elite). The separation was done on a Hypergod C18 column (100 mm by 4.6 mm, 3-µm particle size), with a flow rate of 0.3 ml/min, and then separated on an analytical column (Acclaim PepMap C18, 75 mm by 15 cm) with a linear gradient. The analytical column was heated to 40°C using an AgileSleeve column heater (Analytical Sales and Services), equilibrated with 98% mobile phase A (0.1% formic acid/3% acetonitrile) and 2% mobile phase B (0.1% formic acid/90% acetonitrile), and maintained at a constant column flow of 0.3 ml/min. Sample analysis was performed with SIEVE software (Thermo Fisher Scientific).

Free metabolite detection for glycometabolism

ESCs were pretreated with estrogen (10^{-8} µM) plus progestogen (10^{-6} µM) or indirectly cocultured with JEG3 cells or with primary trophoblast cells (ratio 1:1) for 48 hours and harvested. Glycometabolism in ESCs was determined by LC-MS/MS, as described previously (44). The mass spectrometer used was the 4000 QTRAP System (AB Sciex, Framingham, MA) operated in multiple reaction monitoring mode.

FBP detection

FBP from cells, blood plasma, and tissues were detected using an FBP kit (#BC0920, Solarbio, China) according to the protocol. Cell pellet (ESCs and DSCs) was collected after centrifugation, and tissues (human endometrium and decidua or mouse uterus) were rinsed and weighed; 1 ml of extract solution was added to every 5 million cells or 0.1 g of tissue, and the cells were lysed by ultrasound (ice bath, power 20% or 200 W, ultrasound 3 s, interval 10 s, 30 repetitions), while tissues were ground into a homogenate on ice.

The lysed homogenate was collected and centrifuged at 8000g at 4°C for 10 min, and the supernatant was kept on ice. Reaction reagents were added, and absorbance was measured with a spectrophotometer; the absorbance value was used to calculate the activity of FBP.

Abs for flow cytometry

To identify and evaluate the stromal cells in human endometrium and decidua, the cells were stained with Alexa Fluor 488–conjugated anti-human vimentin Ab (677809, BioLegend). DSCs, trophoblast cells (Tro), DLCs, and dMφs were stained with an Alexa Fluor 488–conjugated anti-human WSX-1/IL-27RA Ab (191106, R&D Systems). Monocytes in peripheral blood, and macrophages in endometrium and decidua were stained with a fluorescein isothiocyanate (FITC)/phycoerythrin (PE)–conjugated anti-human/mouse COX-2 [#13596/#13314, Cell Signaling Technology (CST), USA], allophycocyanin (APC)/Cy7–conjugated anti-human CD45 (368516, BioLegend), and Brilliant Violet 421 (BV421)–conjugated anti-human CD14 Ab (3067144, BioLegend), and dMφs were stained with BV510–conjugated anti-human CD80 (305234), peridinin chlorophyll protein (PerCP)/Cyanine5.5 (Cy5.5)–conjugated anti-human CD86 (374216), PE/Cy7–conjugated anti-human CD163 (333614), APC–conjugated anti-human CD206 (321110), BV421–conjugated anti-human CD209 (330118), PerCP/Cy5.5–conjugated anti-human IFN-γ (502526), PE/Cy7–conjugated anti-human transforming growth factor-β (TGF-β) (349610), Alexa Fluor 488–conjugated anti-human/mouse IRF4 (646405) (all from BioLegend), FITC–conjugated anti-human IDO (eBioscience, 119477-42), PE–conjugated anti-human IL-23p19 (eBioscience, 12-7823-42), and PE–conjugated anti-human IL-12p70 (BD Biosciences, 559325). Human dMφ cells cocultured with ESCs pretreated with FBP or transfected with IL-27 overexpression plasmids were stained with APC/Cy7–conjugated anti-human CD45 (368516), BV421–conjugated anti-human CD14 Ab (3067144), Alexa Fluor 488–conjugated anti-human STAT3 phospho-(Tyr⁷⁰⁵) Ab (651005), and PE–conjugated anti-human STAT3 Ab (371804) (all from BioLegend). Mouse uterus macrophage cells (uMφs) were stained with APC/Cy7–conjugated anti-mouse CD45 (368516), BV421–conjugated anti-mouse F4/80, BV510–conjugated anti-mouse CD80 (104741), FITC/PE–conjugated anti-human/mouse COX-2 [#13596/#13314, CST, USA], PE/Cy5–conjugated anti-mouse CD86 (105016), APC–conjugated anti-mouse CD206 (141708), PE–conjugated anti-mouse CD209 (147801), Alexa Fluor 647–conjugated anti-mouse IDO (647003), PerCP/Cy5.5–conjugated anti-mouse IFN-γ (505822), Alexa Fluor 488–conjugated anti-human/mouse IRF4 (646405), and APC–conjugated anti-mouse IL-10 (505009) (all from BioLegend). Mouse uterus T cells (uT cells) were stained with APC/Cy7–conjugated anti-mouse CD45 (368516), BV421–conjugated anti-mouse CD3 (100228), APC–conjugated anti-human/mouse T-bet (644813), PerCP/Cy5.5–conjugated anti-mouse IFN-γ (505822), Alexa Fluor 488–conjugated anti-human/mouse IRF4 (646405), PE/Cy7–conjugated anti-mouse TNF-α (506323), APC–conjugated anti-mouse IL-10 (505009), PerCP/Cy5.5–conjugated anti-human/mouse GTAT3 (653811) (all from BioLegend), and PE–conjugated anti-mouse ROR-γt (BD Biosciences, 562607). The mouse USCs were stained with an FITC–conjugated anti-mouse vimentin Ab (MB5570210, MyBioSource) and APC–conjugated anti-mouse IL-27p28 Ab (516906, BioLegend).

Western blotting

Western blotting was performed according to the standard procedure to analyze the expression of G6Pase (1:100; Santa Cruz Biotechnology,

#sc25840), HKI (1:100; Santa Cruz Biotechnology, #sc46695), HKII (1:100; Santa Cruz Biotechnology, #sc271459), GPI (1:100; Santa Cruz Biotechnology, #sc374091), PFK1 (1:100; Santa Cruz Biotechnology, #sc377346), FBP1 (1:100; Santa Cruz Biotechnology, #sc271241), ALDO (1:100; Santa Cruz Biotechnology, #sc166918), TPI (1:100; Santa Cruz Biotechnology, #sc166785), glyceraldehyde-3-phosphate dehydrogenase (GAPDH) (1:100; Santa Cruz Biotechnology, #sc47724), PGK1 (1:100; Santa Cruz Biotechnology, #sc130335), PGM1 (1:100; Santa Cruz Biotechnology, #sc373796), PKM (1:100; Santa Cruz Biotechnology, #sc365684), PC-1 (1:100; Santa Cruz Biotechnology, #sc393419), p-c-fos (1:1000; #5348, CST), c-fos (1:1000; #4384, CST), p-ERK (1:1000; #4370, CST), ERK (1:1000; #4695, CST), and β -actin (1:1000; #4970, CST).

Isolation and culture of human ESCs, DSCs, and DLCs

Human ESCs were isolated from the endometrium of healthy control, and DSCs and DLCs were isolated from decidua of women with normal pregnancy according to previously described methods (45). This method provided more than 98% vimentin⁺ CK7⁻ ESCs and DSCs and greater than 98% CD45⁺ DLCs, as confirmed by flow cytometry (FCM) analysis.

Purification of human PBMCs, dM ϕ s, and mouse macrophages

Peripheral blood mononuclear cells (PBMCs) were isolated from the peripheral blood using lymphocyte separation medium (Dakewe, Shenzhen, China). Human dM ϕ s were isolated from decidual immune cells using magnetic beads (Miltenyi Biotec, Bergisch Gladbach, Germany) for in vitro experiments. Mouse macrophages were isolated from the spleen of *Ptgs2*^{-/-} mice or WT mice and further labeled with PKH67 (Sigma-Aldrich, USA) for in vivo experiments.

FBP1-overexpressing ESCs and IL-27-overexpressing ESCs

We obtained FBP1-overexpressing ESCs or IL-27-overexpressing ESCs by transfection with pcDNA(+)-FBP1 or IL-27 plasmids, and the results were confirmed by RT-PCR analysis. The pcDNA(+)-FBP1 or IL-27 plasmids and pcDNA(+)-vector plasmids were from GeneChem Co. Ltd. (Shanghai, China). The ESCs were further cocultured with or without dM ϕ s in vitro.

Construction of G6P-Biotin and FBP-Biotin and HuProt 20K protein array

D-Biotin was directly treated with SOCl₂, and biotin acid chloride was obtained after removal of the excess SOCl₂; the resulting residue was subsequently lyophilized. To a solution of D-glucose 6-phosphate disodium salt hydrate (V900924, Sigma-Aldrich, Germany) or FBP trisodium salt (Sangon Biotech) in DMSO, Et₃N and the above prepared acid chloride (in DMSO) were added dropwise at room temperature. After the reaction reached completion, evaporation and purification yielded the desired product (G6P-Biotin and FBP-Biotin).

After treatment with biotin, FBP-Biotin, and F6P-Biotin, the ESCs were collected, and the sense proteins of FBP were detected by Wayen Biotechnologies Inc. (Shanghai, China) using the HuProt 20K protein array, according to the following procedure (46). The HuProt microarray (CDI Laboratories Inc.) comprises 20,240 human full-length proteins with N-terminal glutathione S-transferase (GST) tags. Human proteome microarrays (HuProt 20K) were blocked with blocking buffer [1% bovine serum albumin and 0.1% Tween 20 in tris-buffered saline and Tween 20 (TBST)] for 1 hour at room temperature with gentle agitation. G6P-Biotin and FBP-Biotin with the Antibody Array Assay Kit (Full Moon Biosystems, Sunnyvale, CA) were

then diluted to 0.01 mg/ml in blocking buffer and incubated on the blocked proteome microarray at room temperature for 1 hour. The microarrays were washed thrice with TBST for 5 min each, incubated with streptavidin-Cy5 at a dilution of 1:1000 (Thermo Fisher Scientific) for 1 hour at room temperature, and subjected to three more 5-min washes. The microarrays were spun dry at 1500 rpm for 3 min and subjected to scanning with a GenePix 4000B (Axon Instruments, Sunnyvale, CA) to visualize and record the results. GenePix Pro 6.0 was used for data analysis. Proteins that may bind to FBP-Biotin are listed in table S1.

Proteomic microarray

After stimulation with FBP (0.5 mM) or without, the supernatants from Ctrl-ESC (secretory phase, *n* = 3) and FBP-ESC (secretory phase, *n* = 3) were collected and analyzed by the proteomic microarray RayBio L-Series Human Antibody Array 1000 (RayBiotech Inc., GA, USA) as described previously (47). The supernatants of IL-27RA⁺ and IL-27RA⁻ dM ϕ s were analyzed similarly.

Enzyme-linked immunosorbent assay

Cytokine concentrations (IL-27) were measured in the supernatants using enzyme-linked immunosorbent assay (ELISA) kits (R&D Systems, USA).

Animals and experimental design

We divided female C57BL/6 mice (8 weeks old, weight: 20 to 23 g) into three groups, using a random number table, by body weight, age, and family; the groups were Ctrl *Il27ra*^{-/-} pregnant mouse group, *Il27ra*^{-/-} pregnant mouse group with adoptive transfer of *Ptgs2*⁺ M ϕ , and *Il27ra*^{-/-} pregnant mouse group with adoptive transfer of *Ptgs2*⁻ M ϕ . This was an unblinded trial.

The differentiation of uM ϕ and uCD4⁺T cells was analyzed by FCM at day 10 of gestation. The transcription levels of *Bmp2*, *Wnt4*, *Hoxa10*, *Cebpb*, *Dprp*, *Igf1p1*, *Ihh*, *Il11*, *Prlr*, and *Lif* in mouse uterus were analyzed by RT-PCR at day 10 of gestation. The primer sequences are described in table S2. The uterine tissues of pregnant mice were labeled with rabbit anti-mouse CK7 Abs for the depth detection of trophoblast invasion by immunofluorescence and immunohistochemical staining at day 10 of gestation. The level of fetal loss was checked at day 14 of gestation in pregnant mice. The day of appearance of a copulatory plug was arbitrarily designated as day 0 of gestation. The embryo absorption rate and implantation number were counted at day 14 of gestation. The percentage of fetal loss (the embryo absorption rate) was calculated as follows: percentage fetal loss = $R/(R + V) \times 100$, where *R* represents the number of hemorrhagic implantation (sites of fetal loss) and *V* stands for the number of viable, surviving fetuses.

For adoptive transfer of macrophages in *Il27ra*^{-/-} pregnant mice, macrophages from spleens of WT mice or *Ptgs2*^{-/-} mice were isolated and purified by magnetic-activated cell sorting, labeled with PKH67, and transferred to *Il27ra*^{-/-} pregnant mice at day 4 of gestation. The uterine tissues of pregnant mice were collected, and depth detection of trophoblast invasion was conducted by immunofluorescence and immunohistochemical staining at day 14 of gestation.

Statistics

Continuous variables are shown as means \pm SEM. They were analyzed by Student's *t* test in case of two groups and by one-way analysis of variance (ANOVA) using Tukey's post hoc test in case of multiple

groups. The embryo resorption rate was analyzed using an adjusted *t* test. All analyses were conducted with SPSS 21.0 software; $P < 0.05$ was considered statistically significant.

SUPPLEMENTARY MATERIALS

Supplementary material for this article is available at <https://science.org/doi/10.1126/sciadv.abj2488>

[View/request a protocol for this paper from Bio-protocol.](#)

REFERENCES AND NOTES

- B. Gellersen, J. J. Brosens, Cyclic decidualization of the human endometrium in reproductive health and failure. *Endocr. Rev.* **35**, 851–905 (2014).
- J. Cha, X. Sun, S. K. Dey, Mechanisms of implantation: Strategies for successful pregnancy. *Nat. Med.* **18**, 1754–1767 (2012).
- T. Garrido-Gomez, N. Castillo-Marco, T. Cordero, C. Simon, Decidualization resistance in the origin of preeclampsia. *Am. J. Obstet. Gynecol.* (2020).
- T. Kajihara, K. Tanaka, T. Oguro, H. Tochigi, J. Prechapanich, S. Uchino, A. Itakura, S. Sucurovic, K. Murakami, J. J. Brosens, O. Ishihara, Androgens modulate the morphological characteristics of human endometrial stromal cells decidualized in vitro. *Reprod. Sci.* **21**, 372–380 (2014).
- J. Evans, L. A. Salamonsen, A. Winship, E. Menkhurst, G. Nie, C. E. Gargett, E. Dimitriadis, Fertile ground: Human endometrial programming and lessons in health and disease. *Nat. Rev. Endocrinol.* **12**, 654–667 (2016).
- A. M. Kelleher, F. J. DeMayo, T. E. Spencer, Uterine glands: Developmental biology and functional roles in pregnancy. *Endocr. Rev.* **40**, 1424–1445 (2019).
- A. Erlebacher, Immunology of the maternal-fetal interface. *Annu. Rev. Immunol.* **31**, 387–411 (2013).
- A. S. Care, K. R. Diener, M. J. Jasper, H. M. Brown, W. V. Ingman, S. A. Robertson, Macrophages regulate corpus luteum development during embryo implantation in mice. *J. Clin. Invest.* **123**, 3472–3487 (2013).
- Y. H. Meng, W. J. Zhou, L. P. Jin, L. B. Liu, K. K. Chang, J. Mei, H. Li, J. Wang, D. J. Li, M. Q. Li, RANKL-mediated harmonious dialogue between fetus and mother guarantees smooth gestation by inducing decidual M2 macrophage polarization. *Cell Death Dis.* **8**, e3105 (2017).
- S. K. Biswas, A. Mantovani, Macrophage plasticity and interaction with lymphocyte subsets: Cancer as a paradigm. *Nat. Immunol.* **11**, 889–896 (2010).
- B. L. Houser, T. Tilburgs, J. Hill, M. L. Nicotra, J. L. Strominger, Two unique human decidual macrophage populations. *J. Immunol.* **186**, 2633–2642 (2011).
- Y. H. Zhang, M. He, Y. Wang, A.-H. Liao, Modulators of the balance between M1 and M2 macrophages during pregnancy. *Front. Immunol.* **8**, 120 (2017).
- M. Chambers, A. Rees, J. G. Cronin, M. Nair, N. Jones, C. A. Thornton, Macrophage plasticity in reproduction and environmental influences on their function. *Front. Immunol.* **11**, 607328 (2020).
- P. S. Minhas, A. Latif-Hernandez, M. R. McReynolds, A. S. Durairaj, Q. Wang, A. Rubin, A. U. Joshi, J. Q. He, E. Gauba, L. Liu, C. Wang, M. Linde, Y. Sugiura, P. K. Moon, R. Majeti, M. Suematsu, D. Mochly-Rosen, I. L. Weissman, F. M. Longo, J. D. Rabinowitz, K. I. Andreasson, Restoring metabolism of myeloid cells reverses cognitive decline in ageing. *Nature* **590**, 122–128 (2021).
- G. Rosenberg, D. Yehezkel, D. Hoffman, C. C. Mattioli, M. Fremder, H. Ben-Arosh, L. Vainman, N. Nissani, S. Hen-Avivi, S. Brenner, M. Itkin, S. Malitsky, E. Ohana, N. B. Ben-Moshe, R. Avraham, Host succinate is an activation signal for *Salmonella* virulence during intracellular infection. *Science* **371**, 400–405 (2021).
- I. Vitale, G. Manic, L. M. Coussens, G. Kroemer, L. Galluzzi, Macrophages and metabolism in the tumor microenvironment. *Cell Metab.* **30**, 36–50 (2019).
- J. H. Lee, R. Liu, J. Li, Y. Wang, L. Tan, X. J. Li, X. Qian, C. Zhang, Y. Xia, D. Xu, W. Guo, Z. Ding, L. Du, Y. Zheng, Q. Chen, P. L. Lorenzi, G. B. Mills, T. Jiang, Z. Lu, EGFR-phosphorylated platelet isoform of phosphofruktokinase 1 promotes PI3K activation. *Mol. Cell* **70**, 197–210.e7 (2018).
- E. D. Tait Wojno, C. A. Hunter, J. S. Stumhofer, The immunobiology of the interleukin-12 family: Room for discovery. *Immunity* **50**, 851–870 (2019).
- J. Zhang, X. Qian, H. Ning, C. S. Eickhoff, D. F. Hoft, J. Liu, Transcriptional suppression of IL-27 production by *Mycobacterium tuberculosis*-activated p38 MAPK via inhibition of AP-1 binding. *J. Immunol.* **186**, 5885–5895 (2011).
- J. Gong, J. Xie, R. Bedolla, P. Rivas, D. Chakravarthy, J. W. Freeman, R. Reddick, S. Kopetz, A. Peterson, H. Wang, S. M. Fischer, A. P. Kumar, Combined targeting of STAT3/NF- κ B/COX-2/EP4 for effective management of pancreatic cancer. *Clin. Cancer Res.* **20**, 1259–1273 (2014).
- A. Lin, G. Wang, H. Zhao, Y. Zhang, Q. Han, C. Zhang, Z. Tian, J. Zhang, TLR4 signaling promotes a COX-2/PGE2/STAT3 positive feedback loop in hepatocellular carcinoma (HCC) cells. *Oncotargets Ther.* **5**, e1074376 (2016).
- Y. Yao, X. H. Xu, L. Jin, Macrophage polarization in physiological and pathological pregnancy. *Front. Immunol.* **10**, 792 (2019).
- M. Dean, Glycogen in the uterus and fallopian tubes is an important source of glucose during early pregnancy. *Biol. Reprod.* **101**, 297–305 (2019).
- R. J. Zuo, X. W. Gu, Q. R. Qi, T. S. Wang, X. Y. Zhao, J. L. Liu, Z. M. Yang, Warburg-like glycolysis and lactate shuttle in mouse decidua during early pregnancy. *J. Biol. Chem.* **290**, 21280–21291 (2015).
- A. I. Frolova, K. O'Neill, K. H. Moley, Dehydroepiandrosterone inhibits glucose flux through the pentose phosphate pathway in human and mouse endometrial stromal cells, preventing decidualization and implantation. *Mol. Endocrinol.* **25**, 1444–1455 (2011).
- J. H. Tsai, M. Schulte, K. O'Neill, M. M. Chi, A. I. Frolova, K. H. Moley, Glucosamine inhibits decidualization of human endometrial stromal cells and decreases litter sizes in mice. *Biol. Reprod.* **89**, 16 (2013).
- A. S. Bhurke, I. C. Bagchi, M. K. Bagchi, Progesterone-regulated endometrial factors controlling implantation. *Am. J. Reprod. Immunol.* **75**, 237–245 (2016).
- C. H. Lee, T. H. Kim, J. H. Lee, S. J. Oh, J. Y. Yoo, H. S. Kwon, Y. I. Kim, S. D. Ferguson, J. Y. Ahn, B. J. Ku, A. T. Fazleabas, J. M. Lim, J. W. Jeong, Extracellular signal-regulated kinase 1/2 signaling pathway is required for endometrial decidualization in mice and human. *PLoS ONE* **8**, e75282 (2013).
- H. R. Christofk, M. G. Vander Heiden, M. H. Harris, A. Ramanathan, R. E. Gerszten, R. Wei, M. D. Fleming, S. L. Schreiber, L. C. Cantley, The M2 splice isoform of pyruvate kinase is important for cancer metabolism and tumour growth. *Nature* **452**, 230–233 (2008).
- K. M. Lee, K. Nam, S. Oh, J. Lim, T. Lee, I. Shin, ECM1 promotes the Warburg effect through EGF-mediated activation of PKM2. *Cell. Signal.* **27**, 228–235 (2015).
- N. Chihara, A. Madi, T. Kondo, H. Zhang, N. Acharya, M. Singer, J. Nyman, N. D. Marjanovic, M. S. Kowalczyk, C. Wang, S. Kurtulus, T. Law, Y. Ertman, J. Nevin, C. D. Buckley, P. R. Burkett, J. D. Buenrostro, O. Rozenblatt-Rosen, A. C. Anderson, A. Regev, V. K. Kuchroo, Induction and transcriptional regulation of the co-inhibitory gene module in T cells. *Nature* **558**, 454–459 (2018).
- D. C. Fitzgerald, G. X. Zhang, M. El-Behi, Z. Fonseca-Kelly, H. Li, S. Yu, C. J. Saris, B. Gran, B. Ciric, A. Rostami, Suppression of autoimmune inflammation of the central nervous system by interleukin 10 secreted by interleukin 27-stimulated T cells. *Nat. Immunol.* **8**, 1372–1379 (2007).
- B. Luan, Y. S. Yoon, J. Le Lay, K. H. Kaestner, S. Hedrick, M. Montminy, CREB pathway links PGE2 signaling with macrophage polarization. *Proc. Natl. Acad. Sci. U.S.A.* **112**, 15642–15647 (2015).
- S. Zhang, Y. Liu, X. Zhang, D. Zhu, X. Qi, X. Cao, Y. Fang, Y. Che, Z. C. Han, Z. X. He, Z. Han, Z. Li, Prostaglandin E2 hydrogel improves cutaneous wound healing via M2 macrophages polarization. *Theranostics* **8**, 5348–5361 (2018).
- H. Lim, B. C. Paria, S. K. Das, J. E. Dinchuk, R. Langenbach, J. M. Trzaskos, S. K. Dey, Multiple female reproductive failures in cyclooxygenase 2-deficient mice. *Cell* **91**, 197–208 (1997).
- H. Wang, S. K. Dey, Roadmap to embryo implantation: Clues from mouse models. *Nat. Rev. Genet.* **7**, 185–199 (2006).
- P. C. Arck, K. Hecher, Fetomaternal immune cross-talk and its consequences for maternal and offspring's health. *Nat. Med.* **19**, 548–556 (2013).
- B. Fu, Y. Zhou, X. Ni, X. Tong, X. Xu, Z. Dong, R. Sun, Z. Tian, H. Wei, Natural killer cells promote fetal development through the secretion of growth-promoting factors. *Immunity* **47**, 1100–1113.e6 (2017).
- H. B. Dias, J. R. de Oliveira, M. V. F. Donadio, S. Kimura, Fructose-1,6-bisphosphate prevents pulmonary fibrosis by regulating extracellular matrix deposition and inducing phenotype reversal of lung myofibroblasts. *PLoS ONE* **14**, e0222202 (2019).
- Y. C. Kim, T. Y. Park, E. Baik, S. H. Lee, Fructose-1,6-bisphosphate attenuates induction of nitric oxide synthase in microglia stimulated with lipopolysaccharide. *Life Sci.* **90**, 365–372 (2012).
- S. M. Seok, T. Y. Park, H. S. Park, E. J. Baik, S. H. Lee, Fructose-1,6-bisphosphate suppresses lipopolysaccharide-induced expression of ICAM-1 through modulation of toll-like receptor-4 signaling in brain endothelial cells. *Int. Immunopharmacol.* **26**, 203–211 (2015).
- F. P. Veras, R. S. Peres, A. L. Saraiva, L. G. Pinto, P. Louzada-Junior, T. M. Cunha, J. A. Paschoal, F. Q. Cunha, J. C. Alves-Filho, Fructose 1,6-bisphosphate, a high-energy intermediate of glycolysis, attenuates experimental arthritis by activating anti-inflammatory adenosinergic pathway. *Sci. Rep.* **5**, 15171 (2015).
- H. Lu, H. L. Yang, W. J. Zhou, Z. Z. Lai, X. M. Qiu, Q. Fu, J. Y. Zhao, J. Wang, D. J. Li, M. Q. Li, Rapamycin prevents spontaneous abortion by triggering decidual stromal cell autophagy-mediated NK cell residence. *Autophagy* **17**, 2511–2527 (2021).
- Y. Li, C. F. Yao, F. J. Xu, Y. Y. Qu, J. T. Li, Y. Lin, Z. L. Cao, P. C. Lin, W. Xu, S. M. Zhao, J. Y. Zhao, APC^{CDH1} synchronizes ribose-5-phosphate levels and DNA synthesis to cell cycle progression. *Nat. Commun.* **10**, 2502 (2019).

45. H. L. Yang, W. J. Zhou, H. Lu, S. T. Lei, S. Y. Ha, Z. Z. Lai, Z. M. Zheng, L. Y. Ruan, Y. Y. He, D. J. Li, M. Q. Li, J. Shao, Decidual stromal cells promote the differentiation of CD56^{bright} CD16⁻ NK cells by secreting IL-24 in early pregnancy. *Am. J. Reprod. Immunol.* **81**, e13110 (2019).
46. T. Zhao, Y. Bao, X. Gan, J. Wang, Q. Chen, Z. Dai, B. Liu, A. Wang, S. Sun, F. Yang, L. Wang, DNA methylation-regulated QPCT promotes sunitinib resistance by increasing HRAS stability in renal cell carcinoma. *Theranostics* **9**, 6175–6190 (2019).
47. J. Mei, W. J. Zhou, X. Y. Zhu, H. Lu, K. Wu, H. L. Yang, Q. Fu, C. Y. Wei, K. K. Chang, L. P. Jin, J. Wang, Y. M. Wang, D. J. Li, M. Q. Li, Suppression of autophagy and HCK signaling promotes PTGS2^{high} FCGR3⁻ NK cell differentiation triggered by ectopic endometrial stromal cells. *Autophagy* **14**, 1376–1397 (2018).

Acknowledgments

Funding: This study was supported by the National Natural Science Foundation of China (NSFC) (nos. 31970798, 81901563, 92057119, 31671200, 81730039, 81671460, 82071646, and 82001636), the National Key Research and Development Program of China (2017YFC1001401 and 2017YFC1001404), the Shanghai Sailing Program (19YF1438500), the Innovation-oriented Science and Technology Grant from NPFPC Key Laboratory of Reproduction Regulation

(CX2017-2), the Program for Zhuoxue of Fudan University (JIF157602), the Support Project for Original Personalized Research of Fudan University (IDF157014/002), and the Open Project Program of Shanghai Key Laboratory of Female Reproductive Endocrine-Related Diseases (grant no. 17DZ2273600). **Author contributions:** W.-J.Z. conducted all experiments and prepared the figures and the manuscript. H.-L.Y. conducted in vivo experiments and prepared the figures and the manuscript. J.M., K.-K.C., H.L., Z.-Z.L., J.-W.S., X.-H.W., and K.W. assisted with sample collection, cell sorting, and in vivo experiments and prepared the figures. T.Z., J.W., and D.-J.L. edited the manuscript. J.-F.Y. assisted with statistics. J.-S.S. assisted with chemical synthesis. M.-Q.L., L.-P.J., and J.-Y.Z. initiated and supervised the project and edited the manuscript. All the authors were involved in writing the manuscript. **Competing interests:** The authors declare that they have no competing interests. **Data and materials availability:** All data needed to evaluate the conclusions in the paper are present in the paper and/or the Supplementary Materials.

Submitted 29 April 2021

Accepted 23 December 2021

Published 23 February 2022

10.1126/sciadv.abj2488

Fructose-1,6-bisphosphate prevents pregnancy loss by inducing decidual COX-2 macrophage differentiation

Wen-Jie ZhouHui-Li YangJie MeiKai-Kai ChangHan LuZhen-Zhen LaiJia-Wei ShiXiao-Hui WangKe WuTao ZhangJian WangJian-Song SunJiang-Feng YeDa-Jin LiJian-Yuan ZhaoLi-Ping JinMing-Qing Li

Sci. Adv., 8 (8), eabj2488. • DOI: 10.1126/sciadv.abj2488

View the article online

<https://www.science.org/doi/10.1126/sciadv.abj2488>

Permissions

<https://www.science.org/help/reprints-and-permissions>

Use of think article is subject to the [Terms of service](#)

Science Advances (ISSN) is published by the American Association for the Advancement of Science. 1200 New York Avenue NW, Washington, DC 20005. The title *Science Advances* is a registered trademark of AAAS.
Copyright © 2022 The Authors, some rights reserved; exclusive licensee American Association for the Advancement of Science. No claim to original U.S. Government Works. Distributed under a Creative Commons Attribution NonCommercial License 4.0 (CC BY-NC).